

## Pyroelectric property of $\text{Pb}(\text{Mg}_{1/3}\text{Nb}_{2/3})\text{O}_3\text{-PbTiO}_3$ ceramics for pyroelectric sensor application

Hak-In Hwang, Jong Man Jung\* and Joon-Shik Park

*Korea Electronics Technology Institute, Pyungtaek 451-860, Korea*

*\*Department of Physics, Dankook University, Cheonan 330-714, Korea*

### 초전센서 응용을 위한 $\text{Pb}(\text{Mg}_{1/3}\text{Nb}_{2/3})\text{O}_3\text{-PbTiO}_3$ 세라믹계의 초전특성

황학인, 정종만\*, 박준식

전자부품 종합기술연구소, 평택, 451-860

\*단국대학교 물리학과, 천안, 330-714

**Abstract** Pyroelectric properties of  $\text{Pb}(\text{Mg}_{1/3}\text{Nb}_{2/3})\text{O}_3\text{-PbTiO}_3$  ceramics prepared by the columbite precursor method have been investigated as a function of the sintering temperature in the range of 1000°C to 1250°C. The  $\text{Pb}(\text{Mg}_{1/3}\text{Nb}_{2/3})\text{O}_3\text{-PbTiO}_3$  ceramics show typical relaxor ferroelectric behavior. The optimum condition for obtaining samples with high densities and improved pyroelectric properties occur at a sintering temperature of 1250°C and sintering time of 2 hours. The  $\text{Pb}(\text{Mg}_{1/3}\text{Nb}_{2/3})\text{O}_3\text{-PbTiO}_3$  ceramics show the possibility for pyroelectric sensors with pyrostat.

**요 약** Columbite precursor 방법을 이용하여 제조한  $\text{Pb}(\text{Mg}_{1/3}\text{Nb}_{2/3})\text{O}_3\text{-PbTiO}_3$  세라믹계의 초전특성을 1000°C에서 1250°C의 소결온도 범위에서 관찰하였다.  $\text{Pb}(\text{Mg}_{1/3}\text{Nb}_{2/3})\text{O}_3\text{-PbTiO}_3$ 계는 전형적인 완화형 강유전특성을 나타내었다. 1250°C에서 2시간 소결한  $\text{Pb}(\text{Mg}_{1/3}\text{Nb}_{2/3})\text{O}_3\text{-PbTiO}_3$  세라믹의 경우, 높은 소결밀도와 향상된 초전특성을 얻을 수 있었다.  $\text{Pb}(\text{Mg}_{1/3}\text{Nb}_{2/3})\text{O}_3\text{-PbTiO}_3$  세라믹은 항온장치를 이용할 경우 초전 센서로의 응용가능성을 나타내었다.

### 1. Introduction

In 1958 Smolenskii and Agranovskaya [1] reported unusual dielectric properties in complex perovskites with the general formula  $\text{Pb}(\text{B}_1\text{B}_2)$  where  $\text{B}_1$  is a low valence cation, e.g.,  $\text{Mg}^{+2}$ ,  $\text{Ni}^{+2}$ ,  $\text{Fe}^{+3}$ , and  $\text{B}_2$  a high valence cation, e.g.,  $\text{Nb}^{+5}$ ,  $\text{Ta}^{+5}$ ,  $\text{W}^{+6}$ . They observed anomalously large and broad dielectric maxima which shifted up in temperature with increasing frequency. Correspondingly, frequency dispersion in the dissipation factor was observed as well. Such characteristic features observed in the so-called relaxor ferroelectric compounds and their solid solutions have attracted special attention for electrostrictive strain application [2-4], electro-optic application [5, 6] and dielectric/pyroelectric bolometers [6].

Among the relaxor ferroelectric materials, lead magnesium niobate ( $\text{Pb}(\text{Mg}_{1/3}\text{Nb}_{2/3})\text{O}_3\text{-PMN}$ ) is the composition with an anomalously large dielectric

constant and a broad diffuse transition temperature of -15°C at 1 kHz measuring frequency [1]. The structure of PMN is pseudo-cubic with space group  $\text{Pm}3\text{m}$  at room temperature [7], with no evidence of long range ordering of the dissimilar B site cation in the  $\text{ABO}_3$  perovskite structure [8]. This disorder in the B site cation is believed to be the basis of relaxor type behavior in such materials [9]. Though the Curie temperature of PMN is well below room temperature, it can be easily shifted upward with  $\text{PbTiO}_3$  (PT) additions, a 'normal' or ordered ferroelectric compound which has a transition at 490°C [10, 11].

In this study, we report the effect of sintering temperature on the stability of perovskite phase and pyroelectric properties of PMN-PT solid solutions.

### 2. Experimental Procedure

Polycrystalline ceramic samples of the  $(1-x)\text{Pb}(\text{Mg}_{1/3}\text{Nb}_{2/3})\text{O}_3-x\text{PbTiO}_3$  were prepared by solid state reaction using the appropriate amount of reagent grade raw materials of  $\text{PbO}$ ,  $\text{MgO}$ ,  $\text{Nb}_2\text{O}_5$  and  $\text{TiO}_2$ . Since it is well known that the formation of perovskite PMN is difficult to fabricate without the appearance of a parasitic pyrochlore phase ( $\text{Pb}_3\text{Nb}_4\text{O}_{13}$ ), the columbite precursor method by Swartz and Shrouf was used [12, 13]. In the first stage a precursor columbite phase,  $\text{MgNb}_2\text{O}_6$ , was prepared by mixing  $\text{MgO}$  and  $\text{Nb}_2\text{O}_5$  in stoichiometric ratio and calcined at  $1000^\circ\text{C}$  for 10 hours. In the second stage, the precursor was mixed in stoichiometric ratios with  $\text{PbO}$  and  $\text{TiO}_2$ . An excess of 0.5 wt%  $\text{PbO}$  was added to compensate for  $\text{PbO}$  volatility during calcining and sintering. The oxides were mixed using attrition milling in distilled water, dried and then calcined at  $850^\circ\text{C}$  for 4 hours. The calcined powder were pressed to form disks followed by sintering from  $1000^\circ\text{C}$  to  $1250^\circ\text{C}$  for 2 hours in closed alumina crucibles. The crystal structure of sintered samples were characterized by X-ray diffractometer (XRD). Microstructural variation of specimens was observed with scanning electron microscopy (SEM). The samples for electrical measurements were prepared from sintered pellets by polishing the faces with SiC grinding paper and electroding with silver paste. The P-E hysteresis loop was investigated using a Sawyer-Tower circuit [14] by applying an AC field of 60 Hz. The pyroelectric coefficient and spontaneous polarization were measured by the static Byer-Roundy method [15] as the samples were heated at a rate of  $4^\circ\text{C}/\text{min}$  through the phase transition. Prior to the electrical measurements each sample was poled by applying a DC field of 2 MV/m at  $-50^\circ\text{C}$  for 30 min.

### 3. Result and Discussion

#### 3.1. Sintering and X-ray Analysis

Figure 1 shows the microstructures of  $(1-x)\text{PMN-xPT}$  ceramics sintered from  $1000^\circ\text{C}$  to  $1250^\circ\text{C}$  for 2 hours. There was remarkable difference in grain size and shapes for the compositions with varying sintering temperature. The SEM micrograph of the sample fired from  $1000^\circ\text{C}$  to  $1150^\circ\text{C}$  revealed a wide distribution of grain sizes and shapes with pores which were mostly located at the grain boundaries

and grain junctions. Increasing the sintering temperature resulted grain growth. The ceramics sintered at  $1250^\circ\text{C}$  showed a dense microstructure with enlarged grains which are substantially free pores. The grain size for the ceramics increased with an increase in sintering temperature and allowed rapid elimination of pores from the samples. A grain size variation of 1 to  $10\ \mu\text{m}$  could be seen (Fig. 1) for the ceramics sintered from  $1000^\circ\text{C}$  to  $1250^\circ\text{C}$ .

X-ray diffractometer was used to examine the formation of pyrochlore phase on the component surfaces. The relative amounts of the pyrochlore and perovskite phase were determined by measuring the major X-ray peak intensities for the perovskite and pyrochlore phase [(110) and (222)], respectively. The percentage of perovskite phase was calculated using the following equation:

$$\text{Perov.}(\%) = \frac{I_{\text{perov.}}}{I_{\text{perov.}} + I_{\text{pyro.}}} \times 100 \quad (1)$$

For all compositions the amounts of perovskite phase was above 88 % for sintering temperature above  $1000^\circ\text{C}$ . The percentage of perovskite phase was summarized in Table 1. The variations in the density of  $(1-x)\text{PMN-xPT}$  ceramics with sintering temperature were shown in Table 1 and Fig. 2. As the sintering temperature increased, the density tended to increase and above  $1150^\circ\text{C}$  reached above 95 % of the theoretical density.

#### 3.2. Physical and Pyroelectric Properties

Figure 3 shows the temperature dependence of the P-E hysteresis loops. As the measurement temperature was increased, the polarization decreased continuously but did not vanish at the phase transition temperature ( $T_c$ ). The temperature dependence of the pyroelectric coefficient and the spontaneous polarization measured by the pyroelectric current were shown in Fig. 4. The spontaneous polarization decreased gradually with increasing temperature, but did not vanish at the phase transition temperature of the solid solution. It was clear that the temperature characteristics of spontaneous polarization showed a typical diffuse phase transition [16]. It was expected that the micro-regions of ferroelectric and paraelectric coexist in the transition region near the transition temperature.

Figures 5 and 6 show the plot of pyroelectric coefficient and spontaneous polarization, respectively,

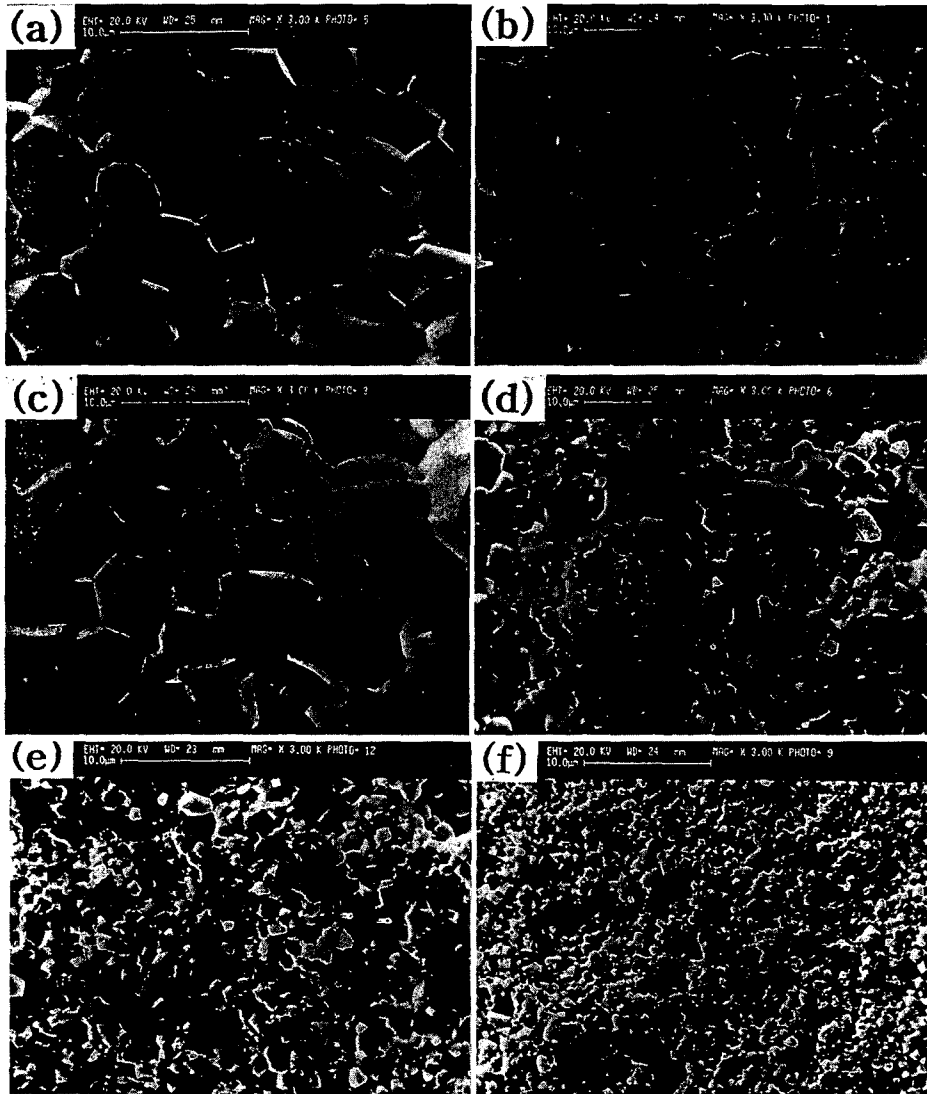


Fig. 1. SEM micrographs for the fracture surfaces of  $(1-x)\text{PMN}-x\text{PT}$  ceramics sintered from  $1000^\circ\text{C}$  to  $1250^\circ\text{C}$  for 2 hours. (a)  $1250^\circ\text{C}$  ( $x=0.03$ ), (b)  $1250^\circ\text{C}$  ( $x=0.07$ ), (c)  $1250^\circ\text{C}$  ( $x=0.09$ ), (d)  $1150^\circ\text{C}$  ( $x=0.09$ ), (e)  $1100^\circ\text{C}$  ( $x=0.09$ ) (f)  $1000^\circ\text{C}$  ( $x=0.09$ ).

for the  $(1-x)\text{PMN}-x\text{PT}$  ceramics sintered at  $1250^\circ\text{C}$  for 2 hours. The maximum value of the pyroelectric coefficient and spontaneous polarization increased with increasing PT mole fraction, and the maximum pyroelectric peak temperature ( $T_p$ ) increased. In the case of PMN the transition temperature was below room temperature. With an addition of PT, phase transition temperature of the  $(1-x)\text{PMN}-x\text{PT}$  could be suitably adjusted for the room temperature pyroelectric and dielectric applications. Pyroelectric coefficient increased with increasing PT for the compositions sintered at  $1250^\circ\text{C}$  for 2 hours. The

ceramics sintered at below  $1250^\circ\text{C}$  showed low pyroelectric properties. The decrease in pyroelectric coefficient with decreasing sintering temperature was ascribed to the increase in amount of grain boundaries which contained the pyrochlore, impurities, etc., which were deterring to pyroelectric coefficients. From this results, it could be shown that the optimum condition for obtaining samples with high densities and improved pyroelectric properties occur at a sintering temperature of  $1250^\circ\text{C}$  and sintering time of 2 hours.

The pyroelectric response of the material was

Table 1  
Dependence of the physical and electrical properties of (1-x)PMN-xPT ceramics on various sintering temperatures

PMN-PT	Sintering Temp. (°C)	T <sub>C</sub> (1 kHz) (°C)	T <sub>P</sub> (°C)	Perov.%	Theo. Density (%)	Max. F <sub>V</sub> (×10 <sup>-3</sup> m <sup>2</sup> C <sup>-1</sup> )	Max. F <sub>D</sub> (×10 <sup>-6</sup> Pa <sup>-1</sup> z)
0.97-0.03	1250	-1	-43	90.9	96.5	12.2	8.96
	1150	7	-44	89.3	95.1	16.2	11.87
	1100	4	-43	89.0	94.6	10.6	7.82
	1050	6	-31	88.9	92.0	12.1	10.09
	1000	7	-35	---	90.9	6.3	4.75
0.95-0.05	1250	12	-47	91.3	96.9	391.6	266.70
	1150	17	--	90.3	95.7	23.2	26.51
	1100	18	-34	89.6	93.7	37.6	29.89
	1050	18	--	90.5	92.9	---	---
	1000	19	-36	90.8	90.8	13.4	10.67
0.93-0.07	1250	24	-22	90.8	96.5	461.4	381.94
	1150	30	-13	90.2	96.1	60.2	50.10
	1100	31	-15	91.1	95.0	32.8	29.44
	1050	31	-15	90.5	93.2	22.8	19.65
	1000	32	-20	89.5	91.1	13.1	10.88
0.91-0.09	1250	35	-5	92.4	96.7	31.7	256.91
	1150	40	--	88.9	95.7	---	---
	1100	42	3	90.9	92.6	26.6	23.92
	1050	42	1	92.3	93.4	17.9	17.29
	1000	42	-1	---	91.1	10.9	10.39

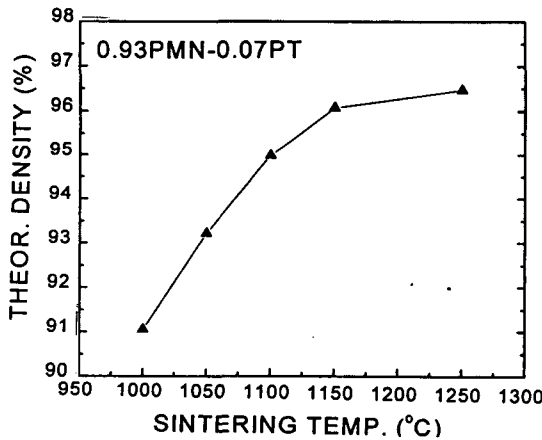


Fig. 2. Density vs. sintering temperature for 0.93PMN-0.07PT ceramic.

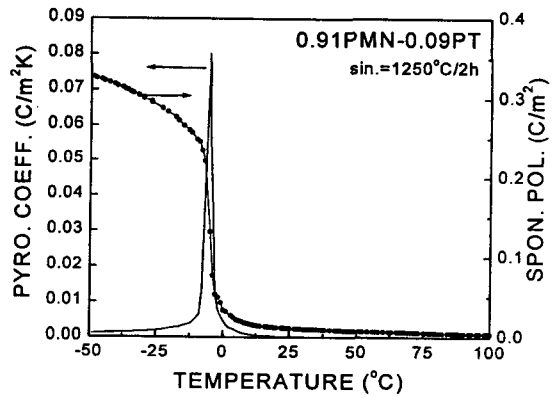


Fig. 4. Temperature dependence of pyroelectric coefficient and spontaneous polarization of 0.91PMN-0.09PT ceramic sintered at 1250°C for 2 hours.

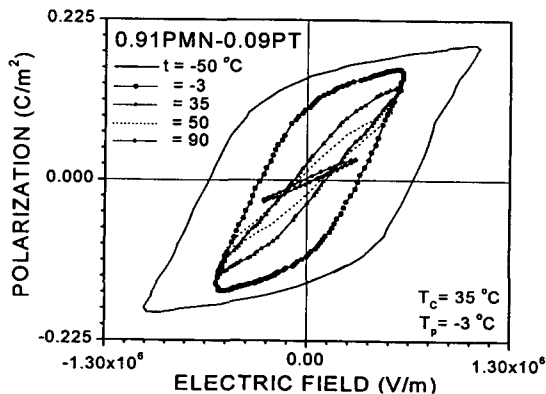


Fig. 3. Plot of polarization vs. electric field of 0.91PMN-0.09PT ceramic.

generally for device application of the figures of merit  $F_V[p/\epsilon_0KC]$  and  $F_D[p/c(\epsilon_0K\tan\delta)^{1/2}]$  [17]. The the maximum  $F_V$  and  $F_D$  of the (1-x)PMN-xPT ceramics showed at Table 1. The dielectric properties of (1-x)PMN-xPT ceramics with varying sintering temperature could be shown in Ref. 18. Figure 7 shows the temperature dependence of  $F_V$  and  $F_D$  for the composition 0.91PMN-0.09PT sintered at 1250°C for 2 hours. The maximum value of pyroelectric figures of merit were obtained at pyroelectric peak temperature. The maximum  $F_V$  and  $F_D$  values of the (1-x)PMN-xPT composition are showed in Table 1. Figure 8 shows the maximum  $F_V$  and  $F_D$  value for the (1-x)PMN-xPT compositions sintered

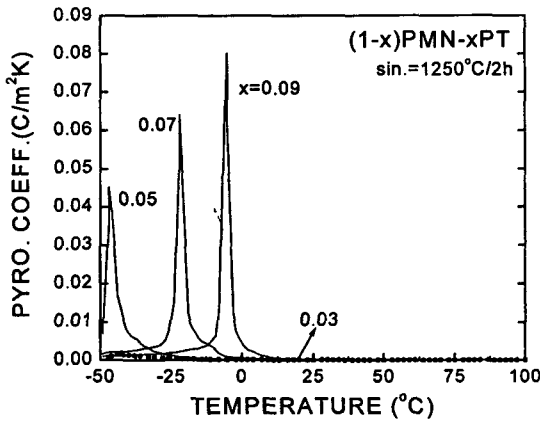


Fig. 5. Temperature dependence of pyroelectric coefficient of (1-x)PMN-xPT ceramics sintered at 1250°C for 2 hours (x=0.03-0.09).

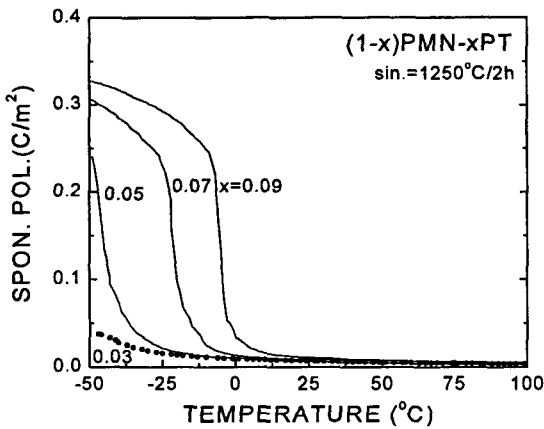


Fig. 6. Temperature dependence of spontaneous polarization of (1-x)PMN-xPT ceramics sintered at 1250°C for 2 hours (x=0.03-0.09).

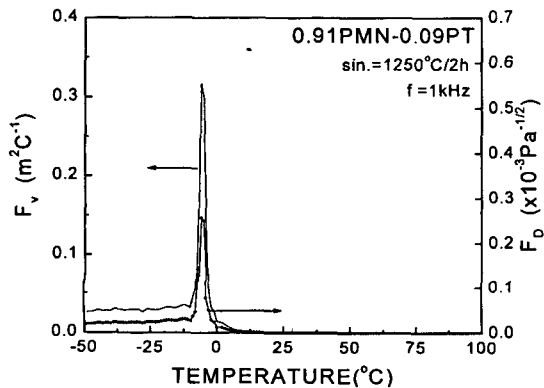


Fig. 7. Temperature dependence of  $F_V$  and  $F_D$  for the composition 0.91PMN-0.09PT ceramic at 1250°C for 2 hours.

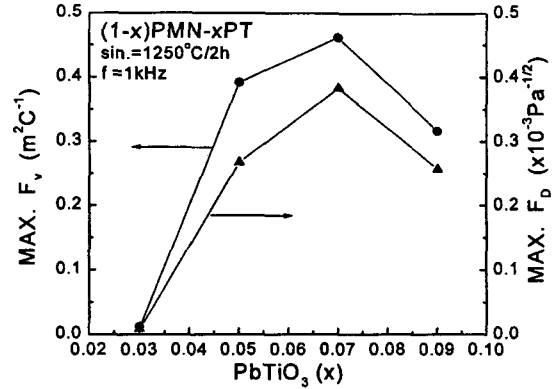


Fig. 8. Maximum  $F_V$  and  $F_D$  value of the (1-x)PMN-xPT ceramics sintered at 1250°C for 2 hours.

at 1250°C for 2 hours. The maximum  $F_V$  and  $F_D$  increased with mole% PT, reached maximum values at 7 mole% PT. However, for x more than ~7 mole%, the maximum  $F_V$  and  $F_D$  value decreased. The maximum  $F_V$  and  $F_D$  value of the composition were comparable to typical value obtained with TGS and  $\text{LiTaO}_3$  [17]. This meant that the (1-x)PMN-xPT system could be used for pyroelectric sensor with pyrostat.

#### 4. Conclusions

(1-x)PMN-xPT ceramics showed a diffuse phase transition. The maximum value of pyroelectric coefficient and spontaneous polarization increased, and the maximum pyroelectric peak temperature moved to higher temperature with increasing PT mole fraction. The optimum condition for obtaining samples with high densities and improved pyroelectric properties occurred at a sintering temperature of 1250°C and sintering time of 2 hours.

The maximum  $F_V$  and  $F_D$  value of the composition were comparable to typical value obtained with TGS and  $\text{LiTaO}_3$ , showed the possibility for pyroelectric sensor with pyrostat.

#### References

- [1] G.A. Smolenskii and A.I. Agranovskaya, Sov. Phys. Tech. Phys. 3 (1958) 1380.
- [2] K. Uchino, S. Nomura, L.E. Cross and S.J. Jang, Ceram. J. Appl. Phys. 51(2) (1980) 1142.
- [3] S.L. Swartz, T.R. Shrout, W.A. Schulze and L.E.

- Cross, *J. Am. Ceram. Soc.* 67 (1984) 311.
- [ 4 ] T.R. Shrout and A. Halliyal, *Am. Ceram. Soc. Bull.* 66(4) (1987) 704.
- [ 5 ] W.A. Bonner, E.F. Dearborn, J.E. Geusic, H.M. Marcos and L.G. Van Uitert, *Appl. Phys. Lett.* 10(5) (1967) 163.
- [ 6 ] R.W. Whatmore, P.C. Osbond and N.M. Shorrock, *Ferroelectrics* 76 (1987) 351.
- [ 7 ] V.A. Bokov and I.E. Myl'nikova, *Sov. Phys. Solid State* 3 (1961) 613.
- [ 8 ] G.A. Smolenskii, V.A. Isupov, A.I. Agranovskaya and S.N. Popov., *Sov. Phys. Solid State* 2 (1961) 2584.
- [ 9 ] W. Wersing, *Ferroelectrics* 7 (1974) 163.
- [10] S.W. Choi, T.R. Shrout, S.J. Jang and A.S. Bhalla, *Mater. Lett.* 8(6,7) (1989) 253.
- [11] S.W. Choi, J.M. Jung and A.S. Bhalla, *Ferroelectrics* 189 (1996) 27.
- [12] S.L. Swartz and T.R. Shrout, *Mat. Res. Bull.* 17 (1982) 1245.
- [13] S.L. Swartz and T.R. Shrout, *Mat. Res. Bull.* 18 (1983) 663.
- [14] H. Diamurt, K. Drenek and R. Pepinsky, *Rev. Sci. Instrum.* 28(1) (1957) 30.
- [15] R.L. Byer and C.R. Roundy, *Ferroelectrics* 3 (1972) 333.
- [16] S.W. Choi, J.M. Jung and A.S. Bhalla, *Ferroelectrics* 189 (1996) 27.
- [17] R.W. Whatmore, A. Patel, N.M. Shorrock and F.W. Ainger, *Ferroelectrics* 104 (1990) 269.
- [18] H.I. Hwang, J.M. Jung and J.S. Park, *Kor. J. Ceram.*: to be published.